The Development of a Dashboard to Optimise Neuromonitoring of Paediatric Traumatic Brain Injury Patients in the Intensive Care Unit

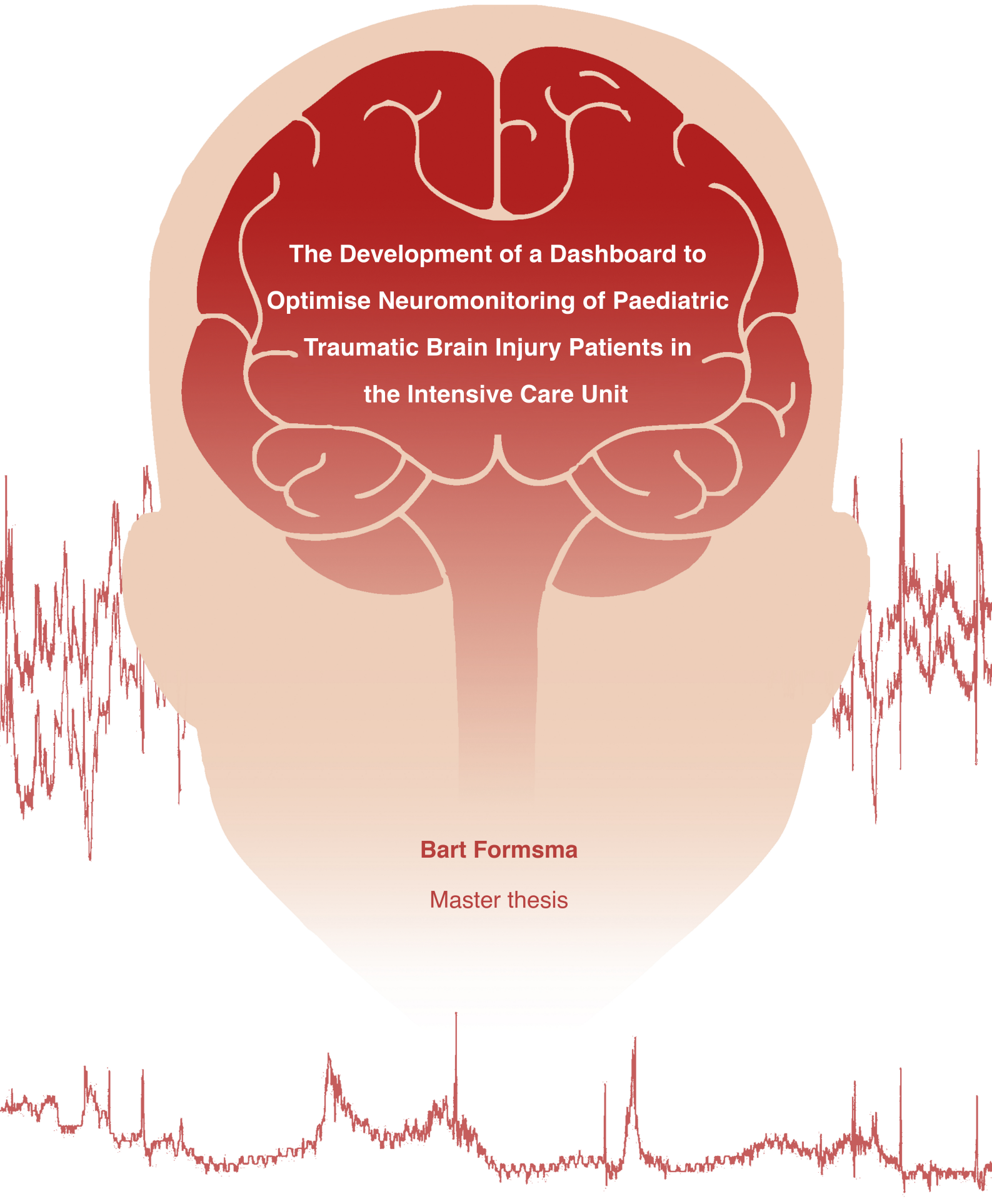

Bart Formsma

Master thesis

The Development of a Dashboard to Optimise Neuromonitoring of Paediatric Traumatic Brain Injury Patients in the Intensive Care Unit

Bart Formsma
Student number: 4438450
December 2022

In partial fulfilment of the requirements for the joint degree of Master of Science in

Technical Medicine

Leiden University | Delft University of Technology | Erasmus University Rotterdam

Master thesis project (TM30004 ; 35 ECTS)

Dept. of Biomechanical Engineering, TUDELFT
March 2022 – December 2022

Supervisor(s):
Prof. dr. ir. A.C. Schouten
Dr. JW Kuiper, MD
Dr. R. de Jonge, MD
drs. E. van Twist

Thesis committee members:

Prof. dr. M. de Hoog, MD (chair)
Prof. dr. ir. A.C. Schouten
Dr. JW Kuiper, MD
Dr. R. de Jonge, MD
drs. E. van Twist

Contents

List of abbreviations

TBI	Traumatic brain injury
PICU	Paediatric intensive care unit
MAP	Mean arterial pressure
ICP	Intracranial pressure
ICP_{cum}	Cumulative intracranial pressure
CPP	Cerebral perfusion pressure
CPP_{opt}	Optimal cerebral perfusion pressure
LLC	Lower limit of optimal cerebral perfusion pressure
ULC	Upper limit of optimal cerebral perfusion pressure
PRx	Pressure reactivity index
wPRx	Wavelet transform pressure reactivity index
WTP	Wavelet transform phase shift
$etCO_2$	End tidal carbon dioxide
P_aO_2	Partial pressure of arterial oxygen
P_aCO_2	Partial pressure of arterial carbon dioxide
PCPC	Paediatric cerebral performance category
AIS	Abbreviation injury scale
PDMS	Patient data management system
F_s	Sampling frequency

Abstract

Introduction Traumatic brain injury (TBI) is a leading cause of childhood morbidity, disability and mortality worldwide. In the treatment of TBI, neuromonitoring is essential to prevent secondary neurological damage. However, the use of neuromonitoring and specifically therapeutic targets is currently limited evidence-based.

Objective The primary objective is to implement suitable neuromonitoring parameters into a novel bedside dashboard for paediatric TBI patients. In addition, basic insights into neuromonitoring parameters between different outcome groups is provided.

Methods Intracranial pressure (ICP), cumulative ICP (ICP_{cum}), cerebral perfusion pressure (CPP), pressure reactivity index (PRx), wavelet transform PRx, optimal CPP (CPP_{opt}), partial pressure of arterial oxygen (P_aO_2), partial pressure of arterial carbon dioxide (P_aCO_2), end-tidal CO_2 ($etCO_2$), temperature and sodium levels were implemented into a dashboard. The parameters (except wPRx) were retrospectively analysed in TBI patients admitted to the paediatric intensive care unit (PICU) of the Erasmus MC- Sophia. Patients were divided into a good (GO) or bad (BO) outcome group. Per outcome group, the mean and 95 % confidence interval or the median and interquartile range of parameters were calculated.

Results A total of 35 patients (24 GO, 11 BO) were included. Significant differences between GO and BO were observed in median PRx (-0.06 [-0.13 – 0.01] vs. 0.17 [-0.05 – 0.39]), median percentage outside of the CPPopt (curve) range (15 % [4 – 26] vs. 30 % [26 – 34]), ICP_{cum} distributions (12.0 mmHg [8.0 – 16.0] vs. 12.0 mmHg [8.5 – 15.5]) and mean sodium levels (146.4 mmol/L (144.5 – 148.3) vs. 151.2 mmol/L (148.6 – 153.8)).

Conclusion In a retrospective analysis, PRx, CPP_{opt}(curve) and ICP_{cum} showed potential to improve prognostication for paediatric TBI and to determine therapeutic targets. Based on our results, we recommend implementing MAP, ICP, ICP_{cum}, CPP alongside CPP_{opt} (curve), and sodium levels in a future neuromonitoring dashboard.

Acknowledgements

First and foremost, I would like to express my sincere gratitude to my supervisors for their continuous support and guidance during my thesis. Jan Willem and Rogier, thank you for giving me the opportunity to work on this project. I really appreciate the elaborate feedback and helping me to keep my focus on finishing my thesis. If it weren't for you, I would still be optimising parameters. Alfred, thank you for the help and advice on the implementation and analysis of the neuromonitoring parameters. I especially enjoyed our discussions about the wavelet transform analysis. Your enthusiasm and critical feedback is much appreciated. Eris, thanks for your endless support and enthusiasm. Before I could take some rest after submitting a draft version, I already received your valuable feedback, always ending on a positive note. I would also like to thank Naomi, for providing a database containing paediatric TBI patient characteristics, and information about the neuromonitoring sensors used in clinical practice.

Finally, I would like to thank my family and friends for their support during this thesis. Especially, I would like to thank my parents, brother and sister for their unconditional support and for providing me a place where I could recover, relieve stress and clear my mind.

1. Introduction

Traumatic brain injury (TBI) is a leading cause of childhood morbidity, disability and mortality worldwide.[1] From 2015 till 2017, 1413 children (18 years or younger) with moderate or severe TBI were administered to Dutch hospitals resulting in an incidence of paediatric TBI of 14 per 100.000 person-years.[2] TBI can be divided into primary and secondary brain injury events. Primary brain injury is irreversible damage caused by mechanical injury at the time of initial injury.[3,4] Secondary brain injury is caused by physiologic responses to the initial injury on a biochemical, cellular and molecular level.[5]

Prevention of secondary brain damage is the key reason to hospitalise paediatric TBI patients.[4] At the paediatric intensive care unit (PICU) of the Erasmus MC Sophia Children's hospital (Rotterdam, the Netherlands), secondary damage is prevented via neuromonitoring on the one hand and, where appropriate, neurosurgical interventions and supportive therapies on the other hand. Therapeutic targets are (1) high/normal blood pressure (age-specific), (2) prevention of hypo- or hyperoxia (p_aO_2 10-15 kPa), (3) prevention of hyperventilation (p_aCO_2 > 4.6-5.0 kPa), (4) maintaining serum sodium levels of 140-150 mmol/L, (5) maintaining an adequate cerebral perfusion pressure (CPP) (age-specific), and (6), if possible, maintaining an intracranial pressure (ICP) below 20 mmHg.[6] However, the use of neuromonitoring and specifically therapeutic targets is currently limited evidence-based. In addition, due to lacking normative paediatric data, there is an absence of therapeutic thresholds based on a favourable patient outcome.[7] Therefore, several paediatric therapeutic targets are derived from adult studies.[7] Paediatric TBI differs from adolescent TBI due to different mechanisms of injury on the one hand, and anatomical and physiological differences on the other hand. Furthermore, even in adults, therapeutic targets remain debatable due to the lack of high-quality evidence.[7,8]

In clinical practice, current monitoring is performed continuously and most data is visualised as a numerical value per second (sampling frequency (F_s) 1 Hz) with limited possibilities to observe both short and long-term trends. In addition, it is not possible to visualise derivatives or combinations of existing neuromonitoring parameters. This diminishes the potential of patient-tailored therapy for paediatric TBI patients. A neuromonitoring dashboard can play an important role in the improvement of neuromonitoring of paediatric TBI patients as it provides a variety of methods to interpret and visualise the measured data, including the trend of the data. In addition, a dashboard enables the possibility to implement additional neuromonitoring parameters and determine therapeutic thresholds in the future.

At the EMC-Sophia PICU, the development of a dashboard displaying parameters of paediatric TBI patients has been initiated. The purpose of this dashboard is to improve both neuromonitoring, therapeutic intervention, and prognostication at the bedside.

The goal of the present study is to improve the novel neuromonitoring dashboard by achieving two subgoals. In a previously written literature review the use of neuromonitoring parameters in paediatric TBI patients is described.[9] They concluded that intracranial pressure (ICP), cumulative ICP (ICP_{cum}), CPP, optimal CPP (CPP_{opt}), partial pressure of arterial oxygen (P_aO_2), partial pressure of arterial carbon dioxide (P_aCO_2), end-tidal carbon dioxide ($etCO_2$) and cerebral temperature are most suitable for implementation into a novel neuromonitoring dashboard aimed at paediatric TBI patients. The first subgoal is to implement the above-mentioned parameters into the current neuromonitoring dashboard. The second subgoal is to perform a retrospective analysis using an existing database of paediatric TBI patients admitted to the PICU of the Erasmus MC- Sophia Children's Hospital to provide basic insights into the differences in neuromonitoring parameters between patients with a good outcome

and patients with a bad outcome. We hypothesize that the neuromonitoring parameters used in the dashboard are significantly different between patient outcome groups and thus can be used to determine therapeutic thresholds.

2. Materials and methods

2.1. Study Population

All paediatric TBI patients admitted to the PICU of the Erasmus MC-Sophia Children's Hospital between January 2016 and September 2022 were evaluated for inclusion in the retrospective analysis. Inclusion criteria were (1) availability of ICP, mean arterial pressure (MAP) and Paediatric Cerebral Performance Category (PCPC) score at 12 months after discharge , and (2) minimum of three hours of continuous monitoring of MAP and ICP. Exclusion criteria were (1) data was interrupted by at least one day of missing data , and (2) the presence of drift artefacts. Patients with missing MAP- and/or ICP-measurements were excluded as several other neuromonitoring parameters require MAP and ICP-data. The decision to exclude patients with less than three hours of continuous MAP and ICP was based on the ICP intensity/duration plots of Guïza et al..[10] They found that the lowest ICP identified (10 mmHg) could be endured for up to 180 minutes before correlating with a worse outcome. Since an ICP of 10 mmHg is commonly encountered in paediatric TBI patients admitted to the EMC – Sophia PICU, the decision was made to set the minimal duration of monitoring to 180 minutes.

Based on a previous literature study of suitable neuromonitoring parameters and the clinical possibilities to measure these parameters at the Erasmus MC-Sophia PICU, the following parameters were considered: MAP, ICP, CPP, pressure reactivity index (PRx), wavelet transform PRx (wPRx), CPP_{opt}, P_aO_2, P_aCO_2, and $etCO_2$.[9] In addition, sodium levels measured by a blood-gas analyser were incorporated in a later stage, as sodium levels enables the possibility to follow the effects of certain medical interventions.[7, A]

Neuromonitoring parameter data was collected from (1) an Erasmus MC server containing monitoring data (Draeger, Lübeck, Germany) and (2) the Patient Data Management System (PDMS) (HiX, Chipsoft, Amsterdam, the Netherlands). In addition, patient characteristics (age and sex), injury severity (Abbreviation Injury Scale (AIS) score), TBI aetiology and outcome (PCPC-score at 12 months after discharge) were collected from a database compiled at Erasmus MC Sophia Children's Hospital (N. Ketharanathan et al.).

2.2 Data Acquisition and Processing

ICP was monitored intraparenchymal using a probe (Codman Microsensor® ICP Transducer, Integra, Princeton, US; Pressio® Catheter, Sophysa, Orsay, France; Camino® Catheter, Nautus Medical Inc., Middleton, US) and continued for as long as was clinically indicated. MAP was monitored invasively through an arterial line (Becton and Dickinson, Franklin Lakes, US). P_aO_2 , P_aCO_2 and sodium-levels were monitored using a blood gas analyser (ABL90 FLEX PLUS, Radiometer Medical ApS, Brønshøj, Denmark). $etCO_2$ was monitored using a non-invasive CO_2 sensor (Dräger, Lübeck, Germany). ICP, MAP, CPP and $etCO_2$ were synchronously recorded at a F_s of 1 Hz.

All processing and analyses were performed using MATLAB (R2021b, The Mathworks, Natick, US). After analysis a visualisation of the conceptual dashboard was created.

[A] An extensive description of the implemented neuromonitoring parameters can be found in the supplementary materials.

Pre-processing

Artefacts were observed in MAP, ICP, CPP and $etCO_2$ samples and were caused by several factors, such as movement of the patient. By removing artefacts in MAP and ICP, artefacts in CPP are also removed since CPP is calculated via subtracting ICP from MAP. Artefacts in MAP, ICP and $etCO_2$ could be identified as sudden pressure shifts to the resting state (0 mmHg) or to values exceeding the pathophysiological normal range.[11]

To determine the pathophysiological range of MAP, ICP and $etCO_2$, raw data of all patients were visualized in separate histograms per parameter. Based on these histograms and expert opinion, thresholds were determined to remove MAP, ICP and $etCO_2$ outliers. To detect artefacts the following conditions were used :

1. Sample is outside the pathophysiological normal range.
2. Sample suddenly increases or decreases compared to the previous sample. (MAP ± 25 %, ICP ± 10 mmHg, $etCO_2$ ± 1 kPa)

Detected artefacts were then replaced by the mean of a 100 sample window (± 50 s). In case the artefacts included the 100 sample window, artefacts were replaced by the values measured before the onset of the artefact.

After artefact removal, MAP, ICP and CPP were low-pas filtered to exclude high frequency waveforms from respiration and pulse rate, by averaging data over 10-second intervals (calculated every 10 s). The F_s of MAP, ICP and CPP after filtering was 0.1 Hz. Figure 1 shows examples of artefact detection, subsequent filtering and data replacement.

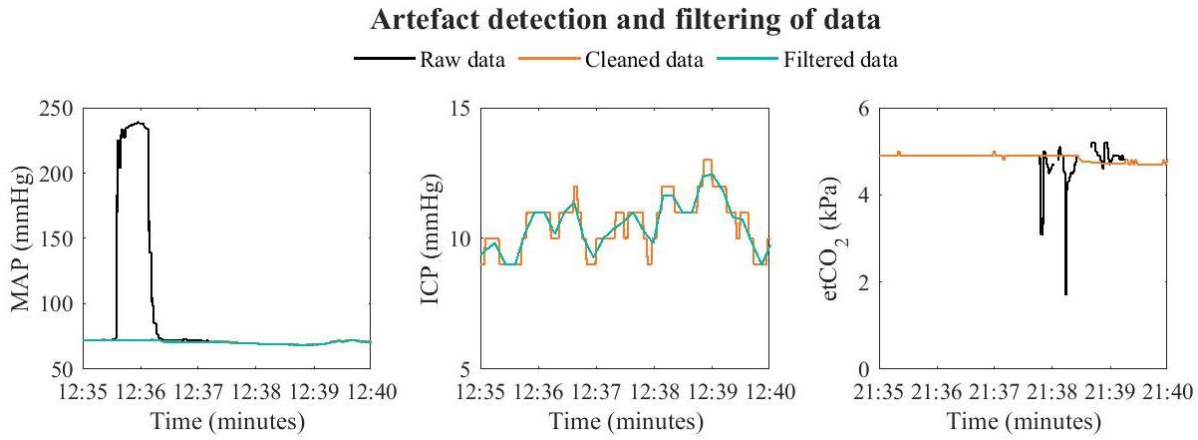

Figure 1: *Artefact detection and filtering of MAP, ICP and $etCO_2$. In the left figure, a large artefact can be observed in the raw MAP data, which is detected, removed and subsequently replaced by mean values. In the middle figure, the filtering of ICP is clearly visualised: the cleaned data is smoothened resulting in filtered data. In the right figure, artefact detection in $etCO_2$ is shown, no filtering occurs, thus the cleaned data is used in further analysis.*

Cumulative Intracranial Pressure

ICP_{cum} was calculated by taking the median ICP-value of each minute interval (6 samples). Subsequently, values were rounded to the nearest integer and the amount of time spent per ICP value was calculated.

Pressure reactivity index

PRx was calculated as the moving Pearson correlation coefficient between 30 consecutive 10 second averages (300 s window, i.e. ± 15 samples) of MAP (F_s 0.1 Hz) and ICP (F_s 0.1 Hz).[12]

Wavelet transform Pressure reactivity index

The wPRx was calculated using the cross wavelet and wavelet coherence toolbox provided by Grinsted et al. as described previously.[13-15] The wPRx was calculated every 10 seconds over an 800 second interval as shown in Figure 2. The wavelet coherence between MAP (F_s 0.1 Hz) and ICP (F_s 0.1 Hz) was calculated in the frequency range of 0.0067 Hz to 0.05 Hz using a Morlet wavelet. In order to remove the edge artefacts, all wavelet coherence values outside of the cone of influence (COI) alongside their corresponding columns were removed. This resulted in the rejection of around 400 seconds of data. In addition, wavelet coherence values with a corresponding wavelet transform coherency below threshold of 0.48 were put to Not a Number (NaN)-values. The threshold of 0.48 was chosen as it has been identified as a threshold to separate signal noise from true physiology.[16] The phase of each scale-frequency point was calculated resulting in the wavelet transform phase shift (WTP) between MAP and ICP. Subsequently the wavelet semblance (cosine of the WTP) was calculated to solve the problem of phase-wrapping and to generate the wPRx. This process produced multiple wPRx values in the 0.0067 Hz to 0.05 Hz frequency range at each time-point (total ~ 400 s). The wPRx values were then averaged along the frequency and time domain to create one wPRx value. An exemplary overview of the calculation of wPRx between two sinusoidal signals is available in Figure 3.

To determine the added value and feasibility of wPRx compared to PRx in a novel dashboard, two sinusoidal signals and data of one patient were analysed. wPRx will be included into the retrospective analysis if the visualisation of cerebral autoregulation was similar between the wPRx and PRx analysis. In case of variation in the visualisation of cerebral autoregulation between PRx and wPRx, wPRx will not be included in the retrospective analysis.

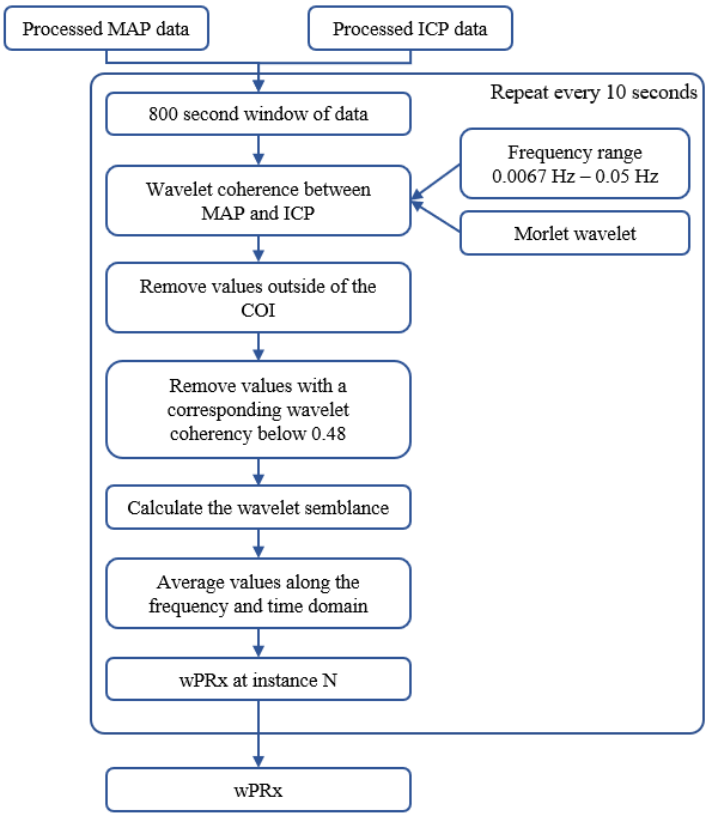

Figure 2: *Flowchart of the calculation of the wavelet transform pressure reactivity index (wPRx). MAP = mean arterial pressure, ICP = intracranial pressure, COI = cone of influence*

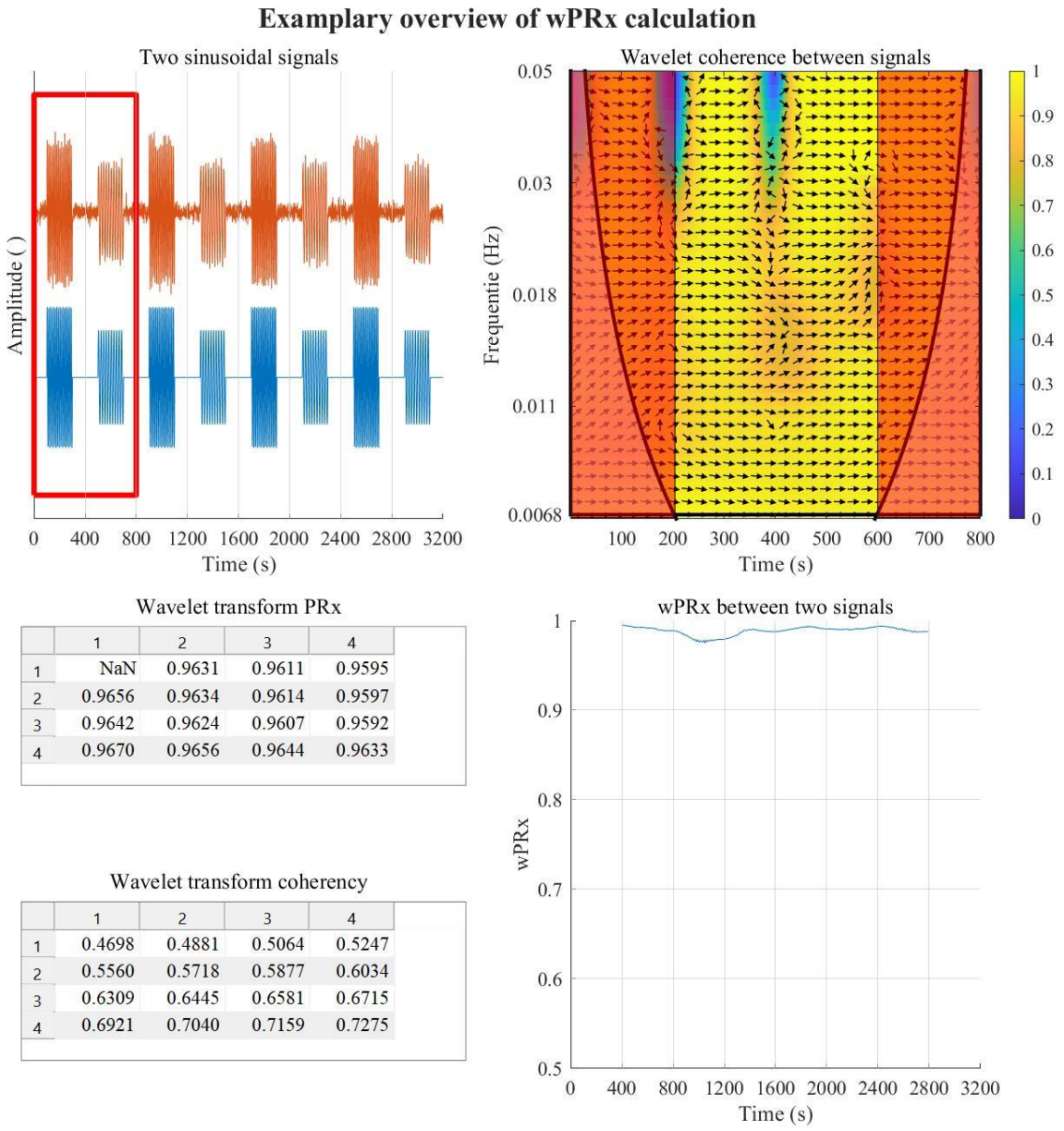

	1	2	3	4
1	NaN	0.9631	0.9611	0.9595
2	0.9656	0.9634	0.9614	0.9597
3	0.9642	0.9624	0.9607	0.9592
4	0.9670	0.9656	0.9644	0.9633

	1	2	3	4
1	0.4698	0.4881	0.5064	0.5247
2	0.5560	0.5718	0.5877	0.6034
3	0.6309	0.6445	0.6581	0.6715
4	0.6921	0.7040	0.7159	0.7275

Figure 3: *Exemplary overview of the calculation of wPRx between two sinusoidal signals.*
1) In the top left figure two sinusoidal signals are shown. The red signal is equal to the blue signal plus noise. The red square marks the 800 second window for the calculation of wPRx. 2) In the top right figure the wavelet coherence between the two signals is shown. Values below the COI (black curved line) and their corresponding columns are removed (red shaded areas). The remaining area is processed resulting in a wPRx matrix. 3) On the bottom left part of the wPRx matrix and corresponding wavelet transform coherency matrix are shown. Note that value (1,1) of the coherency matrix is below 0.48, thus the corresponding wPRx is set to NaN. 4) The wPRx calculation process is repeated every 10 seconds resulting in the bottom right figure.

Optimal Cerebral Perfusion Pressure

CPP_{opt} was calculated over a 4-hour interval and updated every minute as described previously (Figure 4).[17] The mean CPP (F_S = 0.1 Hz) was calculated every minute over a 5 minute interval. Subsequently, the mean PRx (F_S = 0.1 Hz) was calculated every minute over a 1 minute interval. The CPP values were divided into 5 mmHg wide bins alongside their corresponding PRx-values. CPP values of 40 mmHg and 120 mmHg formed the two extreme bins. Per 5 mmHg CPP bin, the mean (μ) of the PRx data was calculated. A second order polynomial curve matching predefined criteria described by Aries et al. was fitted over the data to determine the CPP value with the lowest associated PRx value, labelled CPPbest.[17] If the curve did not met the criteria a NaN-value was assigned to CPPbest.

To determine the lower and upper limit of the CPP_{opt} range two methods were used. In the first method, the lower limit of CPP_{opt} (LLC) and upper limit of CPP_{opt} (ULC) were calculated via subtracting or adding 10mmHg of CPPbest, respectively.[18] In the second method, a PRx threshold of 0.3 was chosen as it has been described as a critical threshold for determining fatal outcome in severe adult TBI patients.[18,19]

Here, LLC and ULC are equal to the intersection points of the threshold and the second order polynomial curve. When the curve did not meet the criteria a NaN value was assigned to CPPbest and no LLC or ULC could be calculated. To achieve a continuous CPP_{opt} range, NaN values were replaced by the mean value of a 100 sample window. When no mean could be calculated due to more than 100 consecutive NaN values, NaN values were replaced by the previously measured value. An exemplary overview of the interactions between CPP and the CPP_{opt} range for a random patient is available in Figure 5.

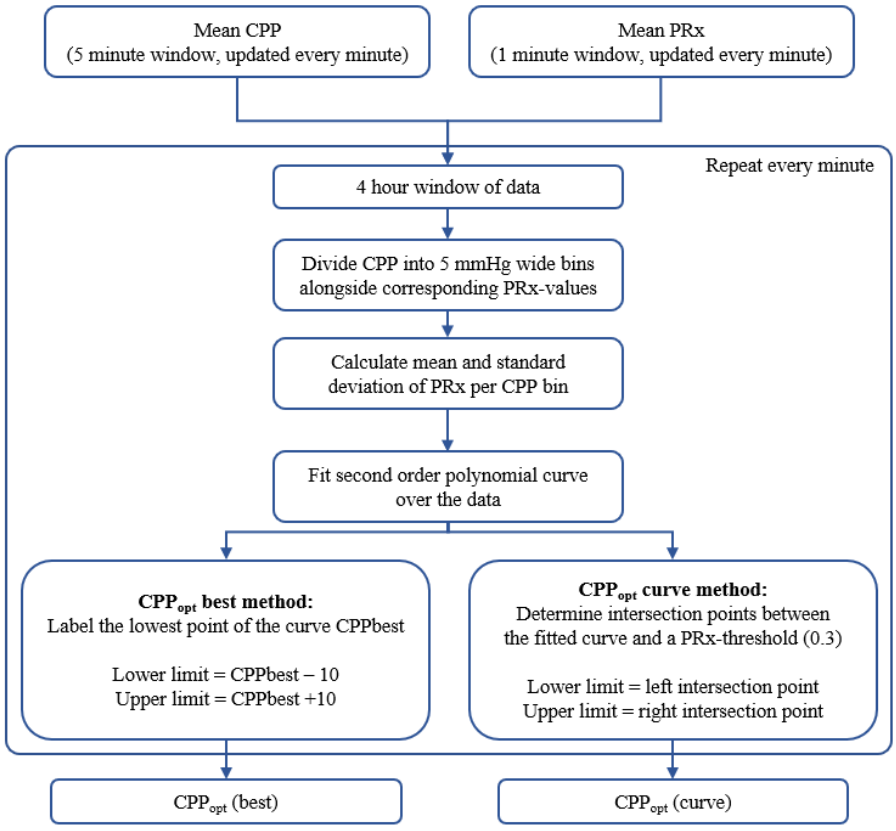

Figure 4: *Flowchart of the calculation of the optimal cerebral perfusion pressure range (CPP_{opt} range). CPP = cerebral perfusion pressure, PRx = pressure reactivity index*

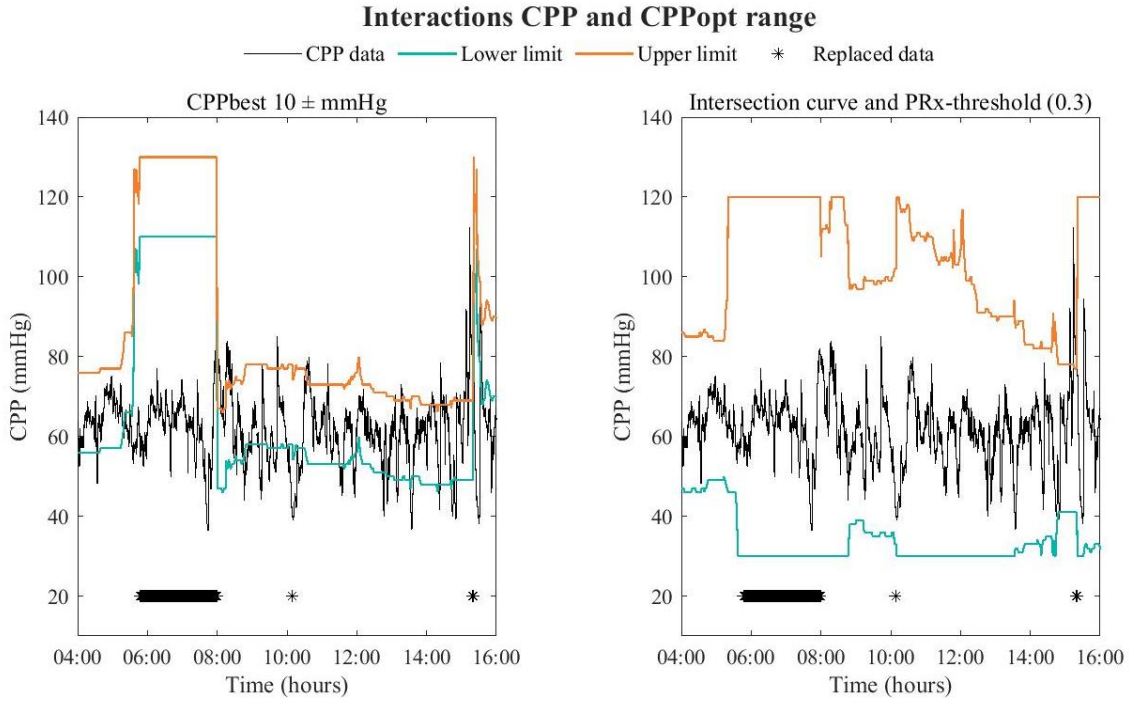

Figure 5: *Interactions between CPP and CPP_{opt} calculated using two methods. Method one is visualised on the left, where the CPPopt range equals CPPbest ± 10 mmHg. On the right side, the CPP_{opt} range using the intersection points between the fitted curve and a predefined PRx threshold of 0.3 is shown. Between 6:00 and 08:00 AM, a constant CPPopt-range can be seen as data is replaced by the previous sample value.*

2.3. Statistical analysis

For each patient the outcome was determined via the PCPC score at 12 months after discharge. The following outcomes were determined per patient to correlate the neuromonitoring parameters to the PCPC-score: parameter data, mean (μ) and/or percentage of data outside the pathophysiological range (if applicable).[20]

To correlate outcome with the neuromonitoring parameters patients were divided into two groups based on their PCPC score at 12 months: a good-outcome group (PCPC 1, 2) and a bad-outcome group (PCPC 3-6). All data were tested for normality using the Shapiro Wilk test. Per outcome group, the mean (μ) and 95% confidence interval (95% CI) were calculated for normal data, while for skewed data the median and interquartile range [IQR] were calculated. Regarding ICP_{cum}, a normalised ICP_{cum} was calculated for both outcome groups. A Student's t-test was performed to compare normally distributed parameters between the two outcome groups. For non-normally distributed parameters a Mann-Whitney U test was performed. A two-sided p-value < 0.05 was considered statistically significant.

3. Results

3.1. Study population and characteristics

A total of 59 patients were eligible for inclusion. Based on the in- and exclusion criteria, a total of 35 patients were included in analysis as depicted in Figure 6.

Based on their PCPC-score, 24 patients were assigned to the good-outcome (GO) group and 11 patients to the bad-outcome (BO) group. Patient and TBI characteristics are shown in Table 1. The median age for the GO- and BO-group were 9.5 years [5.5 – 13.5] and 12 years [9.5 – 15.5], respectively. The total AIS score was 4 [2.4 – 5.6] for the GO-group and 7.5 [4.5 – 10.5] for the BO-group. Furthermore, in 27.2% of the BO-group, TBI was caused by falls compared to 12.5% in the GO-outcome group.

Table 1. *Patient characteristics*

	Good outcome	Bad outcome
Demographics		
Patients	24 (69 %)	11 (31%)
Age years	9.5 [5.5 – 13.5]	12.0 [8.5 – 15.5]
Male	13 (54 %)	5 (45 %)
AIS-score		
Head	4.0 [3.5 – 4.5]	5.0 [4.5 – 5.5]
Total	4.0 [2.4 – 5.6]	7.5 [4.5 – 10.5]
Aetiology TBI		
Bicycle vs car	8 (33,3 %)	4 (36.4 %)
Passenger car accident	3 (12.5 %)	1 (9.1%)
Fall	3 (12.5 %)	3 (27.2 %)
Pedestrian accident	4 (16.7 %)	1 (9.1 %)
Other	2 (8.3 %)	1 (9.1 %)
Unknown	4 (16.7 %)	1 (9.1 %)

Values are represented as N (%) or median [IQR]

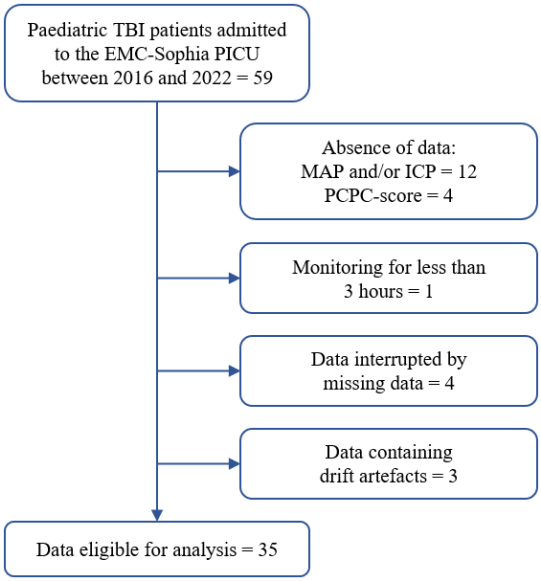

Figure 6: *Patient selection*

3.2. Processing

Pre-processing

Figure 7 shows the histograms of MAP, ICP and $etCO_2$, respectively. Based on these histograms the decision was made to use artefact detection thresholds of 0.01-60 mmHg for ICP, 30-160 mmHg for MAP and 0.01-12 kPa for $etCO_2$.

wPRx

The results of analysing (1) two sinusoidal signals and (2) a paediatric TBI patient using PRx and wPRx are shown in Figures 8 and 9, respectively. Figure 8 shows an exemplary overview of the PRx and wPRx analysis for two sinusoidal signals. The two sinusoidal signals consist of the same alternating sinuses with noise added to one of the signals. As expected, both the PRx as well as the wPRx continuously approximate 1. Note that wPRx is 500 seconds shorter than PRx due to the longer calculation window (800 s vs. 300 s). Figure 9 shows an exemplary overview of the PRx and wPRx analysis for a random patient. Between 15:30 and 16:30 the mean wPRx is positive whilst the mean PRx is negative. Hence, the correlation between MAP and ICP is subjected to variation between PRx and wPRx.

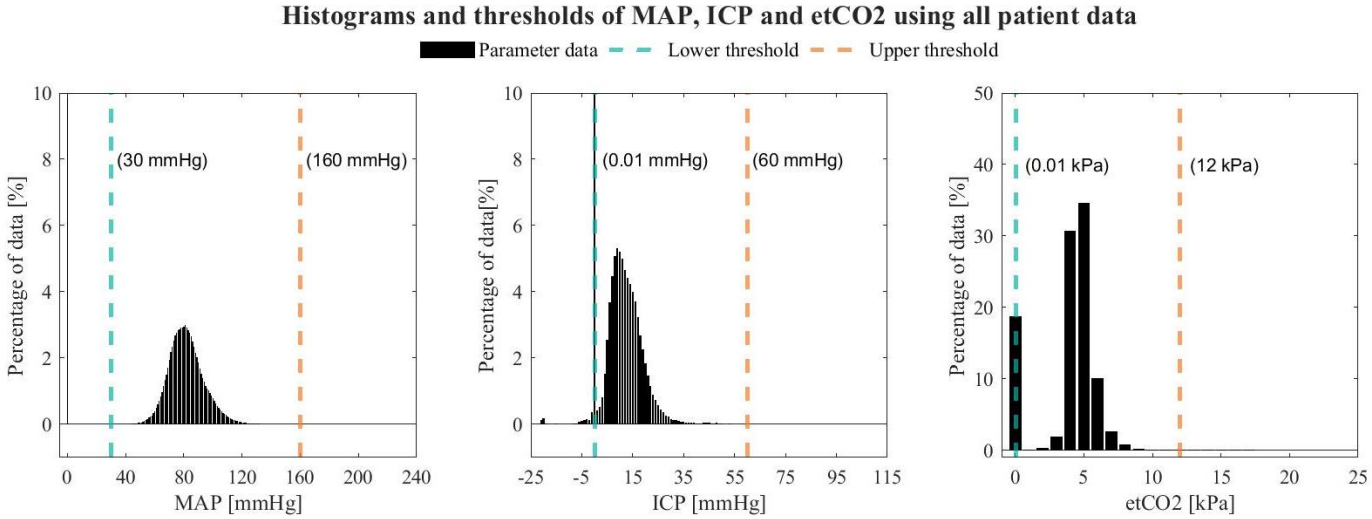

Figure 7: *Histograms and thresholds of MAP, ICP and etCO2. The histograms were made using the raw data of all patients. Note that the x-axis is limited for all histograms to optimise visualisation.*

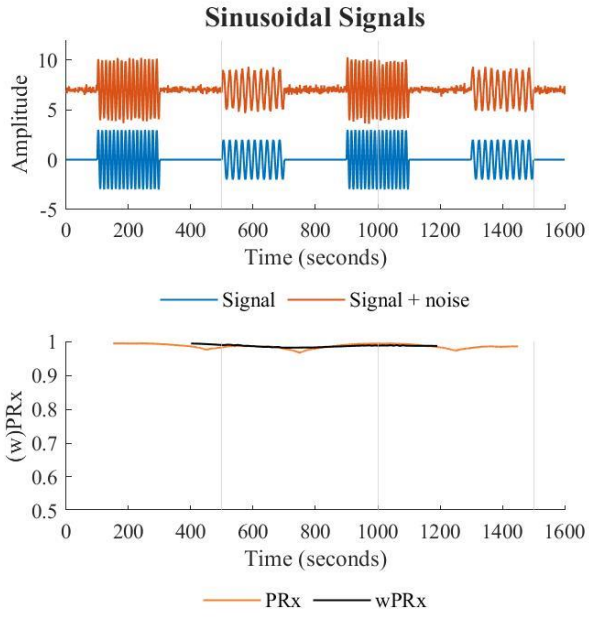

Figure 8: *Exemplary overview of PRx and wPRx analysis for two sinusoidal signals*

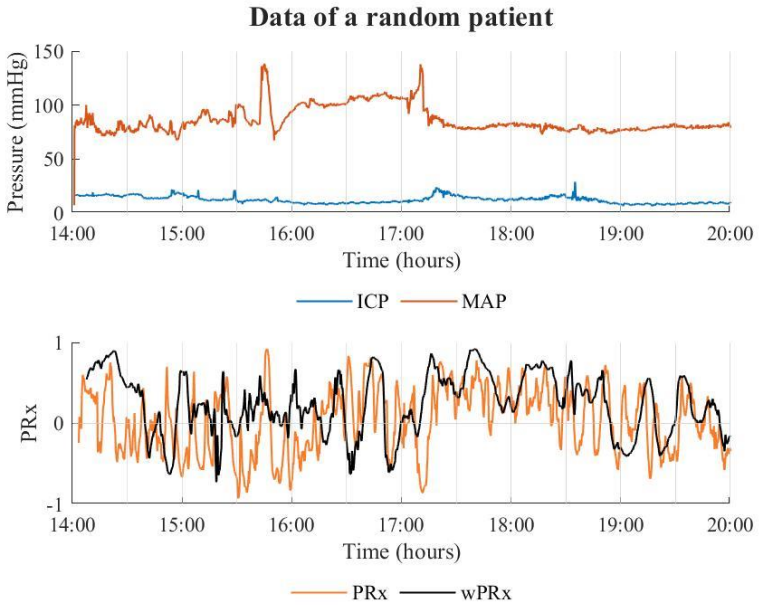

Figure 9: *Exemplary overview of PRx and wPRx analysis for a random patient.*

3.3 Exemplary overview of the neuromonitoring dashboard

Figures 10 and 11 show an exemplary overview of the novel neuromonitoring dashboard for a random patient. MAP, ICP, CPP alongside the CPP_{opt} range, $etCO_2$, p_aO_2, p_aCO_2, serum sodium levels, and temperature were displayed in the TBI overview tab, whereas ICP_{cum} and CPP_{opt} were displayed in the TBI scientific tab.

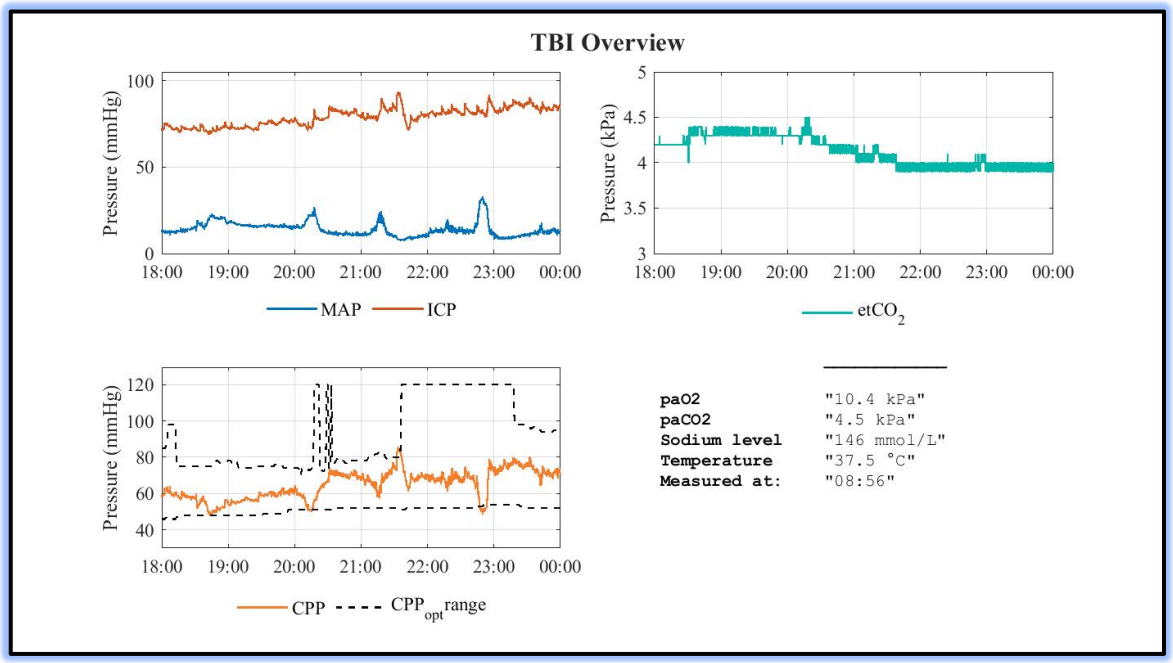

Figure 10: Exemplary overview of the *TBI Overview tab for a random patient. MAP, ICP, $etCO_2$, and CPP alongside the CPP_{opt} range are shown using six hour windows. p_aO_2, p_aCO_2, serum sodium level and temperature were measured at 08:56*

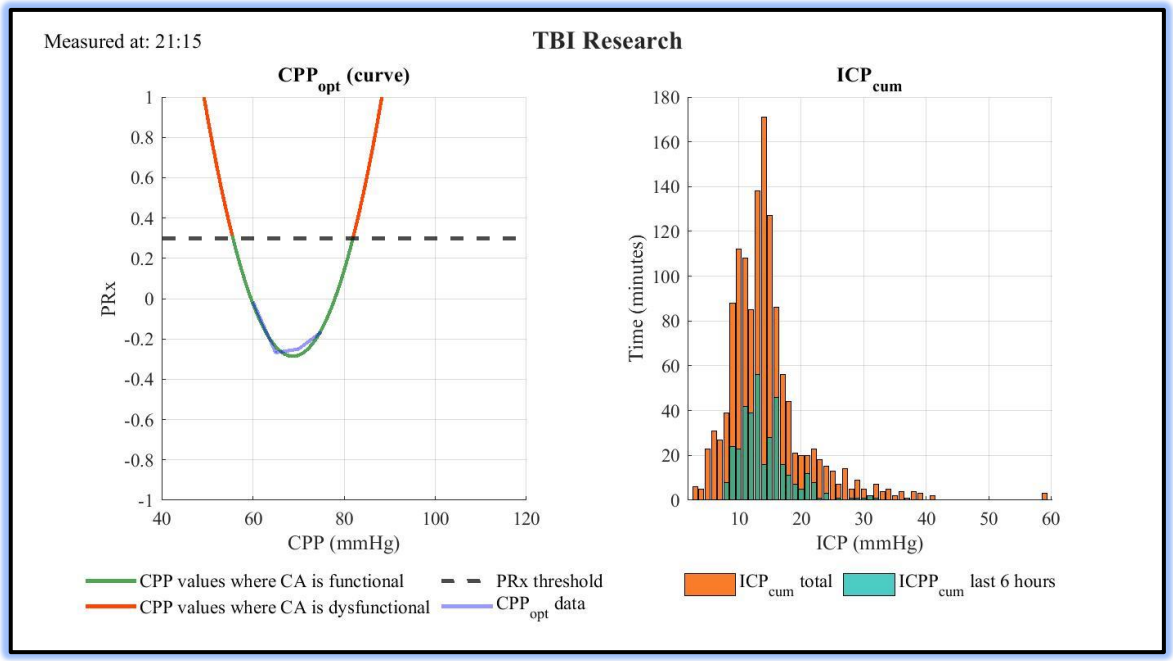

Figure 11: *Exemplary overview of the TBI research tab for a random patient. On the left side, CPP_{opt} is shown using a 4 hour window, i.e. 17:15 – 21:15. The green/red line represents the curve fitted over the CPP_{opt} data. Using the intersection points of the curve and the PRx threshold (0.3), a lower limit of ~55 mmHg and an upper limit of ~80 mmHg can be observed. On the right side ICP_{cum} is shown for the last 6 hours, i.e. 15:15 – 21:15, and for the period from the start of the ICP measurement until the current measurement.*

3.4. Retrospective analysis

The data of MAP, ICP, CPP and sodium levels were normally distributed. Parameters were compared between the GO- and BO- group, see Table 2. Significant differences between the two outcome groups were observed in PRx, CPP_{opt} (curve), ICP_{cum} and sodium levels. Boxplots of the two methods to calculate the CPP_{opt} range are shown in Figure 12. Two contradicting trends can be observed. In CPP_{opt} (curve) the GO-group has a lower median percentage of CPP outside the CPP_{opt} range compared to the BO-group. However, in CPP_{opt} (best) the BO-group has a lower median percentage of CPP outside the CPP_{opt} range compared to the GO-group. The GO-outcome group and BO-outcome group had a ICP_{cum} median of 12 with IQR's of [8.0 – 16.0] and [8.5 – 15.5], respectively. Figure 13 shows the distribution of the average ICP_{cum} per outcome group.

Table 2. Comparison of parameters between outcome groups

	Good outcome	Bad outcome	p-value
MAP, mmHg [A]	79.5 (76.8 – 82.3)	79.9 (76.6 – 83.2)	0.89 [T]
ICP, mmHg [A]	12.3 (11.0 – 13.6)	13.9 (10.8 – 17.0)	0.29 [T]
ICP_{cum}, mmHg [B]	12.0 [8.0 – 16.0]	12.0 [8.5 – 15.5]	0.01 [U]
CPP, mmHg [A]	67.2 (64.7 – 69.7)	66.0 (63.7 – 68.3)	0.55 [T]
PRx [B]	-0.06 [-0.13 – 0.01]	0.17 [-0.05 – 0.39]	0.04 [U]
CPP_{opt}			
Outside CPP_{opt} (best), % [B]	49 [43 – 55]	44 [35 – 53]	0.07 [U]
Outside CPP_{opt} (curve), % [B]	15 [4 – 26]	30 [26 – 34]	0.02 [U]
$etCO_2$, kPa [B]	4.47 [4.08 – 4.86]	4.39 [4.06 – 4.72]	0.74 [U]
p_aCO_2, kPa [B]	4.73 [4.63 – 4.83]	4.58 [4.36 – 4.80]	0.07 [U]
p_aO_2, kPa [B]	11.97 [10.97 – 12.97]	12.15 [11.48 – 12.82]	0.94 [U]
Serum sodium, mmol/L [A]	146.4 (144.5 – 148.3)	151.2 (148.6 – 153.8)	> 0.05 [T]
Temperature, °C [B]	37.0 [36.7 – 37.3]	36.8 [36.6 – 37.0]	0.30 [U]

[A] mean (95% CI) [B] median [IQR] [T] Student's t-test [U] Mann-Whitney U test

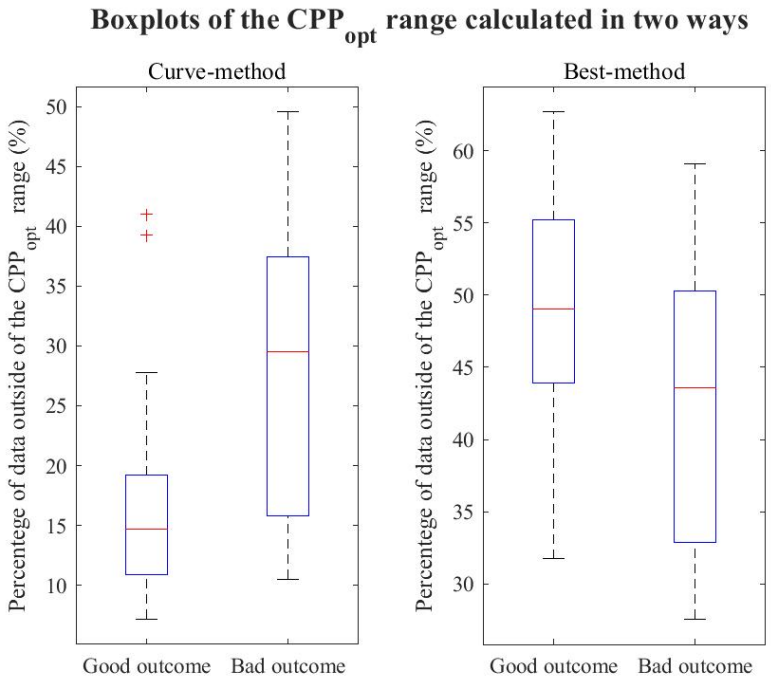

Figure 12: *Boxplots of CPP_{opt} (curve) and CPP_{opt} (Best) for the good and bad outcome group.*

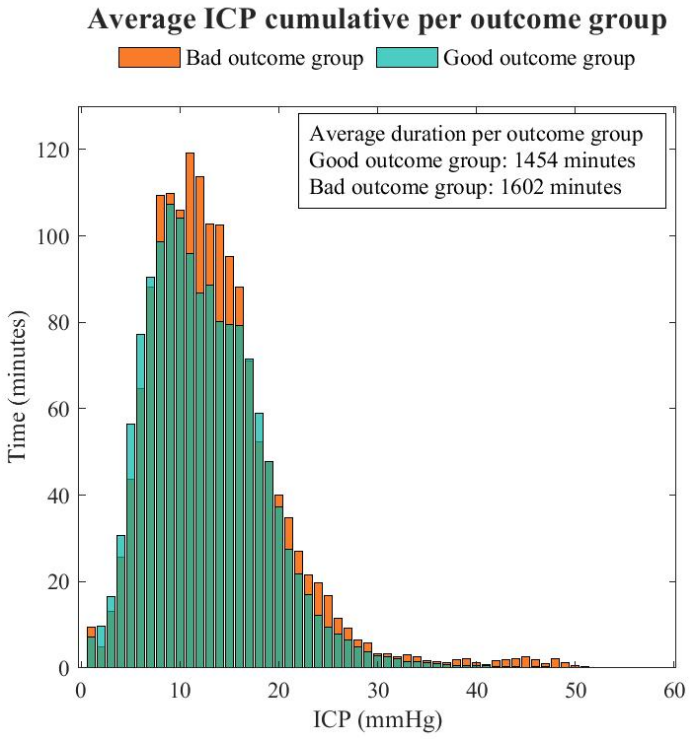

Figure 13: *Distributions of the average ICP cumulative per outcome group. In the textbox, the average duration of ICP monitoring per outcome group is shown.*

4. Discussion

The present study is the first to describe a novel neuromonitoring dashboard specific for the paediatric TBI population. MAP, ICP, CPP, PRx, wPRx, CPP_{opt}, $etCO_2$, p_aCO_2, p_aO_2, serum sodium, and temperature were implemented into the dashboard based on a previously written literature review.[9] In addition, a visualisation of the conceptual dashboard was provided.

The implemented neuromonitoring parameters (with the exception of wPRx) were analysed in 35 paediatric TBI patients who were admitted to the PICU of the Erasmus MC-Sophia Children's Hospital between January 2016 and September 2021. The wPRx was excluded as the results in previous literature could not be reproduced. Comparing patients with a good outcome score (PCPC: 1-2) to patients with a bad outcome score (PCPC: 3-6), revealed significant differences in ICP_{cum}, PRx, CPP_{opt} (curve-method), and sodium levels.

The neuromonitoring dashboard

The novel neuromonitoring dashboard displays MAP, ICP, CPP, PRx, CPP_{opt}, etCO2, paCO2, paO2, sodium, and temperature. In contrast with the current neuromonitoring setting, this dashboard is based on unique derivatives of neuromonitoring parameters, such as CPP_{opt} and PRx. These derivatives visualise the relationship between parameters (e.g. MAP and ICP) which cannot be observed in the current neuromonitoring setting. Furthermore, the derivatives and their trends may provide patient specific therapeutic thresholds. Implementation of patient specific therapeutic thresholds would bypass the current problem of lacking evidence based therapeutic targets due to the absence of normative paediatric data. Hence, implementation of the derivatives into the neuromonitoring of paediatric TBI patients contributes to personalised medicine.

Pre-processing

During pre-processing data were selected for analysis, artefacts were detected and removed, and data were filtered. In data-selection, the length of the parameter data was limited to the length of the period in which both MAP and ICP are calculated. This decision was made since CPP, PRx ,wPRx and CPP_{opt} all require MAP- and ICP-data. In addition, ICP measurements were ceased in case of two scenarios: physiological improvement or all treatment options were exhausted. In both cases, the remaining neuromonitoring parameters are influenced by the scenarios leading to bias.

To detect artefacts in MAP, ICP and $etCO_2$, thresholds were determined using histograms of the raw data of all included patients. For each parameter a histogram was made and interquartile ranges were determined. However these ranges were too narrow and therefore their corresponding thresholds would exclude pathophysiological data. The decision was made to set the lower thresholds of ICP and $etCO_2$ at 0.01 as values equal to or below zero are physiologically impossible. The lower threshold of MAP and the upper thresholds of MAP, ICP and $etCO_2$ were determined based on the histograms in consultation with two paediatric intensivists.

After artefact removal MAP and ICP were low-pas filtered to exclude high frequency waveforms originating from respiration and pulse rate. The $etCO_2$ data were not filtered due to minor influence of respiration and pulse rate and to prevent altering the data. When looking at 6-hour windows, $etCO_2$ is not a smooth signal as it constantly fluctuates between two values with a relatively minor difference for longer periods. The signal could be smoothened via filtering, but this comes with the additional risk of filtering too much.

Neuromonitoring parameters

Cerebral autoregulation enables the brain to compensate for pressure differences caused by traumatic brain injury. In case cerebral autoregulation is affected, the brain is less resistant to pressure changes, causing permanent damage to the brain.[21-24] This could explain why we found an increased PRx and % outside of CPP_{opt} (curve) in patients with a worse outcome (Table 2). Therefore, our results imply but do not prove that cerebral autoregulation is worsened in patients with a PCPC score of 3-6. Similar results have been shown in previous literature between survivor and non-survivor groups, such as research by Donnelly et al. which also showed significant differences in CPP_{opt} (best). [17,18,25,26] However, our study is not directly comparable to Donnelly et al, since they used different outcome groups and a more extensive method to calculate the CPP_{opt} (curve). Instead of using a 4 hour window to calculate CPP_{opt}, multiple windows were applied from a period of 2 hours to 8 hours to determine up to 36 estimations. Subsequently, CPP_{opt} for a single time instance was determined by taking the mean of the estimations. This method provides a more sophisticated calculation of CPP_{opt} making it interesting for future implementation into the neuromonitoring dashboard.

To determine the CPP_{opt} range two methods were used. In both methods a second order polynomial curve matching pre-defined requirements was fitted over the data. In the first method, the lowest point of curve was determined and labelled CPPbest. Subsequently, the lower and upper limit of the CPP_{opt} range were determined by subtracting or adding 10 mmHg, respectively. The second method uses the intersections points between a previously defined PRx-threshold of 0.3 and the second order polynomial curve. To obtain these intersections points the fitted curve was extrapolated over the entire CPP-range used in CPP_{opt} analysis (40-120 mmHg). Due to the extrapolation, the CPP_{opt} range is at some points very wide, reducing sensitivity. On the other hand, CPP_{opt} (best) produces a relatively narrow range, reducing specificity. In both methods missing CPP values are replaced by the moving mean of a 100 sample window. In case the mean could not be calculated the previous sample is used to replace the missing value. Since the CPP_{opt} (best) method covers a smaller range, there is a higher change that CPP is outside of the CPP_{opt} range in case of data replacement. The data replacement is less of a problem for the more wider CPP_{opt} (curve). The lower specificity of CPP_{opt} (best) in combination with the method to replace NaN values could explain why we could not find a significant difference between outcome groups in CPP_{opt} (best).

Based on our results we currently recommend the use of CPP_{opt} (curve) over the use of CPP_{opt} (best) as the prior has shown potential to differentiate between two outcome groups. In addition, data replacement used in artefact detection is less of a problem in CPP_{opt} (curve).

A significant difference was found in the distribution of the average ICP_{cum} between the BO and GO group, where the BO group distribution is shifted to the right compared with the GO group distribution. In addition, ICP data were monitored for a longer average period of time in the BO group. This implies that patients with a bad outcome endured on average higher intracranial pressures for longer periods of time. This is in line with the results of Guïza et al. (2015), who showed that the duration per intensity can be correlated to outcome.[10] Due to the small population size the decision was made to compare the average distributions of the two outcome groups.

The method to calculate wPRx was based on multiple published articles by Liu et al.[14-16] However, their results implying an improved visualisation of cerebral autoregulation by using wPRx compared to PRx could not be reproduced. In addition, calculation of wPRx requires extensive computational power leading to additional costs and analysis time. Therefore, the decision was made to exclude wPRx from the retrospective analysis. However, theoretically the use of wavelet transform analysis is advantageous over the Pearson correlation coefficient making it an interesting method to calculate the pressure reactivity index in future research.

A significant difference in serum sodium levels was found between the two outcome groups, where the BO group had an mean serum sodium level of 151.2 (148.6 – 153.8) mmol/L. Hypernatremia (serum sodium levels > 149 mmol/L) is common in TBI patients and occurs due to several factors such as administering hyperosmotic fluids, limitation of free water or diabetes insipidus.[27,28] Due to the varying causes of hypernatremia it is hard to determine if hypernatremia is correlated to a bad outcome or that patients with a bad outcome develop an iatrogenic hypernatremia. Nonetheless, serum sodium levels are suitable for the dashboard as they enable the possibility to follow the effects of certain medical interventions.[7]

Strengths and weaknesses

In this study, we provided a unique approach to process, calculate, visualise and analyse neuromonitoring parameters and their derivatives to maximise the information acquired from data currently measured in the PICU.

A relatively small population size was available for the retrospective analysis, which precludes a clear correlation between neuromonitoring parameters and outcome. However, small population size is a common occurrence in paediatric neuromonitoring studies. Therefore, most studies divide their patients into survivors and non-survivors. We made the choice to divide the patients into two outcome groups based on PCPC-score (1,2 vs 3-6) due to the relatively small amount of non-survivors (PCPC 6) in our dataset. However, due to the difference in determination of outcome groups, our results are not directly comparable to the results of other studies.

Furthermore, the decision was made to only provide basic insights into the outcome groups using means (95% CI) and medians [IQR] as the main objective was to develop a novel neuromonitoring dashboard. Due to the combination of a small population size and the simple analysing method used, our result only imply but do not prove significant differences in ICP_{cum}, PRx, CPP_{opt} (curve-method), and sodium levels.

Equally important, the current version of the neuromonitoring dashboard is not yet evaluated by a group of clinicians. Before the dashboard can be implemented into the clinical practice, additional research is needed to provide insights into the clinical use of the dashboard by nurses, nurse practitioners and paediatricians. Nonetheless, the neuromonitoring dashboard is suitable for analysis and research purposes.

Clinical implications and Future Perspectives

In clinical practice, current monitoring is performed continuously and most data is visualised as a numerical value per second with limited possibilities to observe both short and long-term trends. In addition, it is not possible to visualise derivatives or combinations of existing neuromonitoring parameters. The neuromonitoring dashboard provides a platform to visualise the shortcomings of the current monitoring, and thus, maximising the information retrieved from the measured data. The dashboard is clinically relevant as it contributes to improvement of the current shortcomings of neuromonitoring. In addition, we provided a framework for future research which is needed to further develop the neuromonitoring dashboard on the one hand, and to implement a novel dashboard into the clinical practice on the other hand.

Regarding the further development of the dashboard, additional research is required to optimise CPP_{opt} and to determine the feasibility of wPRx. The more extensive method described by Donnelly et al. to calculate CPP_{opt} can be implemented and compared with the current method.[18,29] The extensive method may resolve the different trends between CPP_{opt} (curve) and CPP_{opt} (best) and the problem of data replacement. Moreover, wPRx may be worth exploring, as it is a more sophisticated method to quantify relationship between MAP and ICP, which is currently highly susceptible to noise.

Furthermore, multicentre studies can provide a solution to the relatively small population size. This may enable a thorough analysis in survivor and non-survivor outcome groups. In addition, more sophisticated methods such as mixed models can be used to determine differences between outcome groups.

Lastly, additional research is needed to determine how the neuromonitoring dashboard can be implemented into the clinical practice. We recommend to conduct association research between outcomes, and to hold clinical trials to correlate the neuromonitoring dashboard to a possible improvement of the current healthcare.

5. Conclusion

A novel neuromonitoring dashboard for paediatric TBI patients was developed utilizing derivatives and combinations of parameters, such as PRx and CPP_{opt}. Retrospective analysis showed a significant difference in PRx , CPP_{opt}(curve), ICP_{cum} and sodium levels between patients with a good outcome score (PCPC 1&2) and patients with a bad outcome score (PCPC 3-6). As such, PRx , CPP_{opt} (curve), and ICP_{cum} can aid towards paediatric therapeutic targets and improved prognostication. For a future neuromonitoring dashboard we recommend to implement MAP, ICP, ICP_{cum}, CPP alongside CPP_{opt} (curve) and sodium levels. Additional research is required to assess the feasibility of the neuromonitoring dashboard in clinical practice.

References

1. Araki, T., Yokota, H. & Morita, A. Pediatric Traumatic Brain Injury: Characteristic Features, Diagnosis, and Management. *Neurol Med Chir (Tokyo)* **57**, 82-93 (2017).
2. Jochems, D.*, et al.* Epidemiology of paediatric moderate and severe traumatic brain injury in the Netherlands. *European Journal of Paediatric Neurology* **35**, 123-129 (2021).
3. Huffman, J.C., Brennan, M.M., Smith, F.A. & Stern, T.A. Patients with Neurologic Conditions I. Seizure Disorders (Including Nonepileptic Seizures), Cerebrovascular Disease, and Traumatic Brain Injury. (2010).
4. Dohi, K. Pathology and Prevention of Secondary Brain Injury for Neurocritical Care Physicians. in *Neurocritical Care* (ed. Kinoshita, K.) 79-87 (Springer Singapore, Singapore, 2019).
5. Kochanek, P.M.*, et al.* Biochemical, cellular, and molecular mechanisms in the evolution of secondary damage after severe traumatic brain injury in infants and children: Lessons learned from the bedside. *Pediatric Critical Care Medicine* **1**, 4-19 (2000).
6. Ketharanathan N, H.M. Protocol behandeling ernstig neurotrauma op de IC kinderen. (ed. Hospital, E.M.S.C.s.) (Erasmus MC Sophia Children's Hospital, 2021).
7. Kochanek, P.M.*, et al.* Guidelines for the Management of Pediatric Severe Traumatic Brain Injury, Third Edition: Update of the Brain Trauma Foundation Guidelines. *Pediatric Critical Care Medicine* **20**(2019).
8. Carney, N.*, et al.* Guidelines for the Management of Severe Traumatic Brain Injury, Fourth Edition. *Neurosurgery* **80**, 6-15 (2016).
9. Formsma, B. Neuromonitoring parameters in paediatric traumatic brain injury patients: an overview. (2022).
10. Güiza, F.*, et al.* Visualizing the pressure and time burden of intracranial hypertension in adult and paediatric traumatic brain injury. *Intensive Care Medicine* **41**, 1067-1076 (2015).
11. de Jonge, S. Development of a dashboard for the clinical use in patients with severe neurotrauma on the paediatric intensive care. (2021).
12. Czosnyka, M.*, et al.* Continuous assessment of the cerebral vasomotor reactivity in head injury. *Neurosurgery* **41**, 11-17; discussion 17-19 (1997).
13. Grinsted, A., Moore, J.C. & Jevrejeva, S. Application of the cross wavelet transform and wavelet coherence to geophysical time series. *Nonlin. Processes Geophys.* **11**, 561-566 (2004).
14. Liu, X.*, et al.* Cerebrovascular pressure reactivity monitoring using wavelet analysis in traumatic brain injury patients: A retrospective study. *PLoS Med* **14**, e1002348 (2017).
15. Liu, X.*, et al.* Wavelet Autoregulation Monitoring Identifies Blood Pressures Associated With Brain Injury in Neonatal Hypoxic-Ischemic Encephalopathy. *Front Neurol* **12**, 662839 (2021).
16. Liu, X.*, et al.* Wavelet pressure reactivity index: a validation study. *J Physiol* **596**, 2797-2809 (2018).
17. Aries, M.J.*, et al.* Continuous determination of optimal cerebral perfusion pressure in traumatic brain injury. *Crit Care Med* **40**, 2456-2463 (2012).
18. Donnelly, J.*, et al.* Individualizing Thresholds of Cerebral Perfusion Pressure Using Estimated Limits of Autoregulation. *Crit Care Med* **45**, 1464-1471 (2017).
19. Sorrentino, E.*, et al.* Critical thresholds for cerebrovascular reactivity after traumatic brain injury. *Neurocrit Care* **16**, 258-266 (2012).
20. Nenadovic, V.*, et al.* Fluctuations in cortical synchronization in pediatric traumatic brain injury. *J Neurotrauma* **25**, 615-627 (2008).

21. Raboel, P.H., Bartek, J., Andresen, M., Bellander, B.M. & Romner, B. Intracranial Pressure Monitoring: Invasive versus Non-Invasive Methods–A Review. *Critical Care Research and Practice* **2012**, 950393 (2012).
22. Smith, M. Monitoring Intracranial Pressure in Traumatic Brain Injury. *Anesthesia & Analgesia* **106**, 240-248 (2008).
23. Wilson, M.H. Monro-Kellie 2.0: The dynamic vascular and venous pathophysiological components of intracranial pressure. *J Cereb Blood Flow Metab* **36**, 1338-1350 (2016).
24. Young, A.M.H*., et al.* Multimodality neuromonitoring in severe pediatric traumatic brain injury. *Pediatric Research* **83**, 41-49 (2018).
25. Brady, K.M*., et al.* Continuous monitoring of cerebrovascular pressure reactivity after traumatic brain injury in children. *Pediatrics* **124**, e1205-1212 (2009).
26. Young, A.M*., et al.* Continuous Multimodality Monitoring in Children after Traumatic Brain Injury-Preliminary Experience. *PLoS One* **11**, e0148817 (2016).
27. Kolmodin, L., Sekhon, M.S., Henderson, W.R., Turgeon, A.F. & Griesdale, D.E. Hypernatremia in patients with severe traumatic brain injury: a systematic review. *Ann Intensive Care* **3**, 35 (2013).
28. Azovskiy, D., Lekmanov, A., Pilyutik, S. & Gegueva, E. *Hypernatremia in pediatric patients with severe traumatic brain injury*, (Crit Care. 2010;14(Suppl 1):P291. doi: 10.1186/cc8523. Epub 2010 Mar 1., 2010).
29. Depreitere, B*., et al.* Pressure autoregulation monitoring and cerebral perfusion pressure target recommendation in patients with severe traumatic brain injury based on minute-by-minute monitoring data. *J Neurosurg* **120**, 1451-1457 (2014).
30. DeMers D, W.D. Physiology, Mean Arterial Pressure. Vol. 2022 (StatPearls Publishing, Treasure Island (FL), StatPearls [Internet], 2021).
31. Sun, J., Yuan, J. & Li, B. SBP Is Superior to MAP to Reflect Tissue Perfusion and Hemodynamic Abnormality Perioperatively. *Front Physiol* **12**, 705558-705558 (2021).
32. Gomes, J.A. & Bhardwaj, A. CHAPTER 4 - Normal Intracranial Pressure Physiology. in *Cerebrospinal Fluid in Clinical Practice* (ed. Irani, D.N.) 19-25 (W.B. Saunders, Philadelphia, 2009).
33. Czosnyka, M. & Pickard, J.D. Monitoring and interpretation of intracranial pressure. *Journal of Neurology, Neurosurgery & Psychiatry* **75**, 813-821 (2004).
34. Mount CA, M.D.J. Cerebral Perfusion Pressure. Vol. 2022 (StatPearls Publishing, Treasure Island (FL), StatPearls [Internet], 2021).
35. White, H. & Venkatesh, B. Cerebral Perfusion Pressure in Neurotrauma: A Review. *Anesthesia & Analgesia* **107**, 979-988 (2008).
36. Tameem, A. & Krovvidi, H. Cerebral physiology. *Continuing Education in Anaesthesia Critical Care & Pain* **13**, 113-118 (2013).
37. Kelly, S., Bishop, S.M. & Ercole, A. Statistical Signal Properties of the Pressure-Reactivity Index (PRx). *Acta Neurochir Suppl* **126**, 317-320 (2018).
38. Steiner, L.A*., et al.* Continuous monitoring of cerebrovascular pressure reactivity allows determination of optimal cerebral perfusion pressure in patients with traumatic brain injury. *Critical Care Medicine* **30**, 733-738 (2002).
39. Czosnyka, M., Czosnyka, Z. & Smielewski, P. Pressure reactivity index: journey through the past 20 years. *Acta Neurochir (Wien)* **159**, 2063-2065 (2017).
40. Tas, J*., et al.* Targeting Autoregulation-Guided Cerebral Perfusion Pressure after Traumatic Brain Injury (COGiTATE): A Feasibility Randomized Controlled Clinical Trial. *J Neurotrauma* **38**, 2790-2800 (2021).

41. Collins, J.-A., Rudenski, A., Gibson, J., Howard, L. & O'Driscoll, R. Relating oxygen partial pressure, saturation and content: the haemoglobin-oxygen dissociation curve. *Breathe (Sheff)* **11**, 194-201 (2015).
42. Hantzidiamantis, P.J. & Amaro, E. Physiology, Alveolar to Arterial Oxygen Gradient. in *StatPearls* (StatPearls Publishing

43. Razi, E., Moosavi, G.A., Omidi, K., Khakpour Saebi, A. & Razi, A. Correlation of end-tidal carbon dioxide with arterial carbon dioxide in mechanically ventilated patients. *Arch Trauma Res* **1**, 58-62 (2012).
44. Doppmann, P.*, et al.* End-tidal to arterial carbon dioxide gradient is associated with increased mortality in patients with traumatic brain injury: a retrospective observational study. *Sci Rep* **11**, 10391 (2021).
45. Zhang, Z., Guo, Q. & Wang, E. Hyperventilation in neurological patients: from physiology to outcome evidence. *Curr Opin Anaesthesiol* **32**, 568-573 (2019).
46. Citerio, G.*, et al.* Management of arterial partial pressure of carbon dioxide in the first week after traumatic brain injury: results from the CENTER-TBI study. *Intensive Care Med* **47**, 961-973 (2021).
47. Messina Z, P.H. Partial Pressure of Carbon Dioxide. Vol. 2022 (StatPearls Publishing, Treasure Island (FL), StatPearls [Internet], 2021).
48. Edwards, S.L. Pathophysiology of acid base balance: the theory practice relationship. *Intensive Crit Care Nurs* **24**, 28-38; quiz 38-40 (2008).
49. Curry, B.W., Ward, S., Lindsell, C.J., Hart, K.W. & McMullan, J.T. Mechanical Ventilation of Severe Traumatic Brain Injury Patients in the Prehospital Setting. *Air Medical Journal* **39**, 410-413 (2020).

Supplementary materials

Neuromonitoring parameters [9]

Mean arterial pressure (MAP)

As the heart contracts, it pumps blood into the vascular system, i.e. cardiac output. The cardiac output (CO) in combination with systemic vascular resistance (SVR) generates a systolic and a diastolic pressure from which MAP is derived. MAP is the pressure gradient driving the blood perfusion of organs to maintain their functioning. It can be influenced by changes in CO and SVR, which themselves are reliant on multiple variables. The pressure can be estimated by taking the mean pressure over a systole and diastole. Formulas 1 and 2 can be used to estimate MAP.[30]

1) $MAP = DBP + \frac{1}{3} \times (SBP - DBP)$
2) $MAP = DBP + \frac{1}{3} \times (PP)$

Where DBP is equal to diastolic blood pressure, SBP is equal to systolic blood pressure, and PP is equal to pulse pressure. Whereas MAP can reflect changes in CO, SBP can reflect changes in stroke volume. In addition, SBP can reflect haemodynamic changes, the perfusion of organs, and the heart's systolic function.[31]

Intracranial pressure (ICP) and Cumulative ICP (ICP_{cum})

ICP is the pressure generated by fluids within the cranium relative to the atmospheric pressure.[32] According to the Monroe-Kellie doctrine, ICP is derived from the relationship between changes in the volumes of CSF and cerebral blood, and the ability of the craniospinal compartment to compensate for these changes.[22,32] In this relationship, also known as spatial compensation, the CSF component of ICP is responsible for baseline ICP. In addition, small continuous fluctuations can arise on top of the baseline ICP, caused by the vasogenic component.[22] When CSF and/or cerebral blood cannot be reduced adequately, an increase in ICP may be provoked. This can occur in pathological conditions such as cerebral oedema, lesions, and obstruction of the CSF circulation.[33]

ICP episodes can be visualised via the cumulative ICP (ICP_{cum}), which shows the total duration spent per ICP intensity. As Such, ICP_{cum} gives a personalised distribution per patient.

Cerebral Perfusion Pressure (CPP)

CPP is the net pressure gradient that drives CBF, i.e. oxygen delivery to cerebral tissue. In a healthy situation, the ICP is relatively low (5-10 mmHg) and so CPP is mainly dependent on MAP.[34] When the MAP changes, cerebral autoregulation ensures that CPP and CBF remain relatively constant through changes in CVR. This relationship can be described by CBF=CPP/CVR. Normal CPP levels are needed to maintain an adequate CBF. [35,36]

Pressure Reactivity Index (PRx)

PRx represents the cerebrovascular pressure reactivity and can be used to approximate cerebral autoregulation. The PRx is calculated by taking the Pearson correlation coefficient between the slow waves of ICP and MAP.[37] When cerebral autoregulation is intact, ICP will reduce or remain constant in response to an increased MAP. Hence, the PRx will be zero or negative.[37,38] By contrast, impaired cerebral autoregulation will result in a positive PRx.

Wavelet transform Pressure Reactivity Index (wPRx)

One of the biggest disadvantages of PRx is that it is a very noisy parameter due to physiological variability of MAP and ICP.[16,39] A more appropriate method to quantify the noisy relation between MAP and ICP is the wPRx, which uses a wavelet-transform analysis. [16]

Optimal Cerebral Perfusion Pressure (CPP_{opt})

CPP_{opt} is a dynamic patient-tailored parameter derived from the relationship between CPP and PRx. Plotting PRx against CPP will result in an U-shaped curve. The lowest point of this curve represents the CPP value with optimal autoregulatory capacity, i.e. CPP_{opt}.[29,40] In comparison with CPP, CPP_{opt} takes patient's physiology and age-specific parameters into account.

Arterial partial pressure of Oxygen (P_AO_2)

The partial pressure of a gas in a liquid can be described as "the equivalent to the partial pressure which would prevail in a gas phase in equilibrium with the liquid at the same temperature".[41] P_aO_2 is determined by the alveolar partial pressure of oxygen (PAO_2) minus the alveolar-arterial gradient, i.e. the difference between PAO_2 and P_aO_2. The alveolar-arterial gradient is partially determined by a physiological mismatch between ventilation and perfusion in the lungs.[42]

P_aO_2 itself is an important determinant of arterial oxygen saturation (S_aO_2), i.e. the fraction of haemoglobin bound by oxygen. P_aO_2 and S_aO_2 can be related to each other via the oxygen-haemoglobin dissociation curve (ODC). An increase in P_aO_2 is accompanied by an increase in S_aO_2, but in different proportions. Once S_aO_2 reaches 100%, an increase in P_aO_2 cannot lead to an increase in S_aO_2. Hence, oxygen will dissolve directly into the blood.

Arterial partial pressure of Carbon Dioxide (P_ACO_2) & End Tidal Carbon Dioxide ($ETCO_2$)

Carbon dioxide (CO_2) is a waste product of the aerobic metabolism. It is transported via blood to the lungs, where it is cleared through ventilation. Here, $EtCO_2$ represents the body's ability to clear CO_2. Hence, $EtCO_2$ can provide an indication for cardiac output, pulmonary blood flow and P_aCO_2. In mechanically ventilated patients, $EtCO_2$ can be used as surrogate for P_aCO_2.[43] However, the difference between them, i.e. the CO_2 gap, is determined by the physiological and alveolar dead space. In ventilated patients the CO_2 gap is generally around 3.8 mmHg. In contrast, the CO_2 gap can be very inconsistent in patients with impaired alveolar ventilation.[44]

P_aCO_2 plays an important role in both the balance of the respiratory system and in the cerebrovascular tone.[45-47] Respiratory wise, P_aCO_2 is the primary controller of minute ventilation. In general, an increase in P_aCO_2 causes a decrease in pH, i.e. a more acidic environment. Subsequently, these changes lead to an increase in minute ventilation to clear P_aCO_2.[47] Simultaneously, the increased P_aCO_2 causes cerebral vasodilatation, which leads to an increased CBV and CBF. The increase in intracranial volume could eventually raise the ICP.[45,46] On the other hand a decrease in P_aCO_2 causes an increase in pH, i.e. a more alkaline environment. [48] This will lead to a decrease in minute ventilation and cause cerebral vasoconstriction.[47,48] Due to cerebral vasoconstriction, CBV and CBF will decrease. A decrease in CBF is associated with the risk of secondary ischaemic insults. [46] Overall, both a decreased and an increased P_aCO_2, i.e. hypocapnia and hypercapnia, are associated with increased mortality.[45,46,49]